COBEM 2021 26th International Congress of Mechanical Engineering
November 22-26, 2021, Virtual Congress, Brazil

# COBEM2021-1094
# MECHANICAL DESIGN OF A REDUCED FZG TRIBOMETER WITH VARIABLE LOADING

**Lenine Marques de Castro Silva**
**Aylla Maria de Moura Alencar Rocha**
**Adilson José de Oliveira**
**Salete Martins Alves**

Federal University of Rio Grande do Norte (UFRN) - Lagoa Nova Campus – Natal, RN, Brazil - Zipcode 59078-900
leninemcs@ufrn.edu.br
ayllaalencar9@hotmail.com
adilson@ct.ufrn.br
saletealves@ect.ufrn.br

***Abstract.*** *This work presents a detailed mechanical design of a reduced FZG test rig based on the tribometer according to DIN ISO 14635-1:2000. The standardized FZG tribometer consists of two parallel gearboxes (one driving and the other driven) connected by two parallel shafts forming a back-to-back power recirculation system. However, this system has considerable limitations for academic applications, such as (1) the necessity of 1.25 liters of fresh oil per box at each test; (2) the load application is carried out statically; and, therefore, (3) a non-viability of an automated test. Aiming to resolve the described issues, this work aimed: (i) to plan a scale reduction that shall require no more than 100 ml of fresh oil per gearbox; (ii) to design a parallel loading system based on a disk brake system and coupled at a third shaft; and (iii) to add an electric motor drive system triggered by a frequency inverter. According to the modifications, the new mechanical design allows: (a) the variation of the load without stopping the machine; (b) simultaneous tests on two gears pairs under the same conditions; (c) the use of cylindrical helical gears; (d) the automation of the test; and (e) the application of dynamic loading by mechanical actuators.*

***Keywords:*** *mechanical design, gears tribology, FZG test; oil load capacity; variable load*

## 1. INTRODUCTION

Gearboxes are widely used in mechanical power transmission systems. They function to change the angular speed and torque on the input shaft concerning the output shaft, keeping power constant. In the Brazilian Rio Grande do Norte state (e.g.), gearboxes have been used to convert wind into electrical energy. The referred Brazilian state has more than 150 installed wind farms with a total power of 4,043.1 GW (ABEEólica, 2019). In a typical situation, the rotation speed caused by the wind to the turbine blades (20 rpm) is not enough for the conversion, and speed multiplier gearboxes are used to reach 1620 rpm (Fernandes et al., 2016).

In wind turbines, electrical and electronic components present more failures than mechanical ones (Santos et al., 2016). However, the industry efforts are concentrated on understanding the mechanical components failures modes because the downtime due to a mechanical failure is more significant than that due to an electrical or electronic failure (Spinato et al., 2009).

The mechanical failures on gears are intrinsically linked to the lubrication efficiency and the deterioration of the lubricant film between the gears' teeth. The Technical University of Munich developed a test rig to study the load capacity of lubricant films to prevent mechanical failures on spur gears teeth. The equipment was denominated FZG test rig, and it was standardized by DIN ISO 14635-1:2000.

The described standard presents a tribometer composed of two gearboxes working in parallel and interconnected by two shafts. The test rig is driven by an electric motor and, to accelerate the gears' failures, there is also a load system coupled to one of the shafts. Nevertheless, considerable limitations can be observed in the FZG test rig. Firstly, the size of the components (gears housing and gears) demands the use of 1.25 l of lubricant per gearbox in each test. This need precludes the operation with lubricants with limited production (e.g., lubricant oils with nano additives). In addition, the charge is statically added to the system, which is a constraint factor in gears test rigs based on power recirculation (Manoj *et al.*, 2015). In other words, the electric motor has to be turned down so that the new load can be applied on the shafts and, consequently, on the gears' teeth. That operation mode hinders the automation of the test once it requires an operator to couple the lever arm on the shaft and applies the standard mass..

Then, this work aims to redesign the FZG test rig to attenuate the limited conditions aforementioned. In the first place, a scale reduction was proposed with the view to the volume of lubricant oil required by each test. The main

objective of this design change is to test small amounts of lubricant oil, which have limited production. The second point addresses the change of the load system from a static application with a lever arm and using standard mass to a charger that can vary the load during the test procedure. Thus, several improvements can be explored from this change, i.e.: (i) the variation of the load in a continuous test (with no need to stop the electric motor); (ii) the realization of simultaneous tests using both gearboxes as test gearboxes; (iii) the possibility to automate the test procedure with the aid of a programmable logic controller; and (iv) the future possibility of applying dynamic charges with the aid of a mechanical actuator in replacing the standard masses triggering the disk brake system.

The reduced FZG test rig shall be supported on a rigid metal frame capable of bearing the weight of the tribometer and the vibration stemming from the machine operation. The metal frame shall also be versatile and for receiving new sub-assemblies as future upgrades to the system. Moreover, the reduced test rig shall count on a mechanical torque limiter, indicating possible overcharges coming from the electric motor. Furthermore, the reduced FZG test rig shall run tests in cylindrical helical gears without the change of the bearings (the possibility that is not left by DIN ISO 14635-1:2000). Lastly, the new test rig mechanical design shall foresee positions for transducers to monitor in real-time the variation of others parameters (e.g., the lubricant oil temperature, the shafts angular position, the shafts angular velocity, and the system vibration levels).

## 2. PROJECT PREREQUISITES

The main propose of this study was to redesign a typical FZG tribometer capable of inducing wear on the gears' teeth flanks lubricated by amounts of oil limited to 100 ml (maximum) in each gearbox. It was also aimed to implement improvements at points described before as limitations of the original FZG. Then, this work followed a bottom-up project strategy. The subassemblies were designed according to the functional need. The gearboxes were the first subassemblies to be designed, followed by subassemblies involving shafts, load system, torsional spring coupling, metal frame, and electric motor drive system.

The development of each subassembly was based on clear criteria, which analyze the relevance for the system. The criteria were: (*i*) functional need; (*ii*) performance; (*iii*) operational facility; (*iv*) operational safety; and (*v*) maintenance. So, the creation process of the subassemblies took into account the presented criteria, and a summarized analysis is shown in Fig. 1.

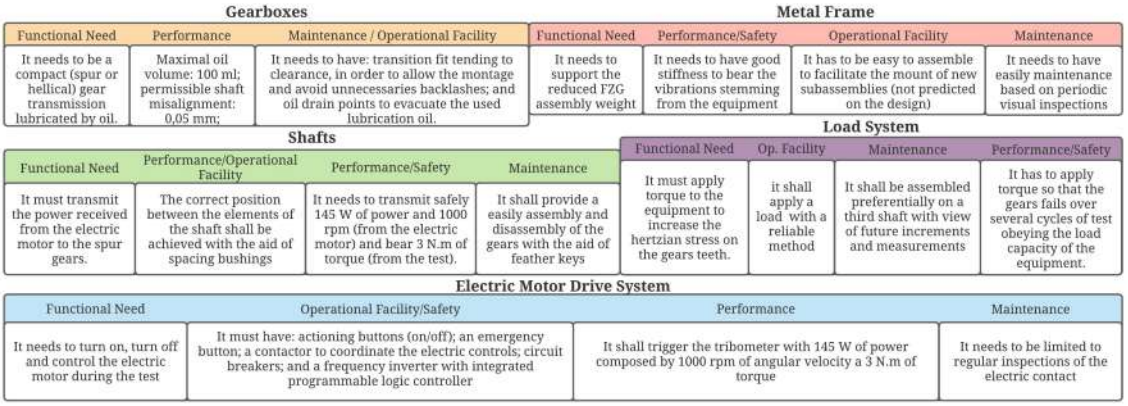


Figure 1. Project criteria for the designed subassemblies.

In order to facilitate the manufacturing phase, this project: (i) selected standard mechanical parts which are commercialized in the Brazilian market; (ii) designed mechanical parts which can be machined with standard tools (turning inserts, drills, reamers, taps and mills). Thus, the standardized parts were the rolling bearings, seal retainer, housed bearings, couplings, feather keys, and of course, gears. On the other hand, the parts that must be manufactured at the university lab are the shafts, bearings housing, gear housing, flange, and spacing bushings.

The mechanical parts exclusively dedicated for new propose needed to go through a conception sequence, i.e.: (*i*) 3D modeling in the CAD system; (*ii*) engineering analysis; (iii) elaboration of technical drawings for manufacturing processes; (v) planning the manufacturing processes. The CAx platform Creo Parametric® 6.0 was used during the product development phase.

According to DIN ISO 14635 (2000), the lubrication mode suitable for this case is the splash lubrication, and the oil level shall be up to three times the gear tooth height (Carreteiro e Belmiro, 2006). Meanwhile, the required lubricant volume must not be greater than 100 ml, so the tests can be feasible to limited production of lubricant oils.

The shafts shall be designed based on three prerequisites: (*i*) they need to fit in the selected gears; and, meeting the first condition, (*ii*) their diameter and selected material shall facilitate the ensuing construction and bear the work conditions.

## 3. GEARBOXES AND SHAFTS DESIGN

To meet the gears project requirements and to make then easily accessible in order to facilitate test preparation, the selected gears are broadly commercialized by A.T.I. Brasil (a Brazilian national supplier specialized in power transmission industrial parts). Gears model BE401010040 and the BE401010028, manufactured of AISI 1045 steel, were selected to fulfill requisites (ATI Brasil, 2021). So, the gears have the features presented in Tab. 1:

Table 1. Selected gears features.

| | z [-] | m [mm] | dp [mm] | ϕ [°] | t [mm] | β [°] | E [GPa] |
|---|---|---|---|---|---|---|---|
| **Pinion (1)** | 28 | 1 | 28 | 20 | 7 | 0 | 206.8 |
| **Gear (2)** | 40 | | 40 | | | | |

Where z, m, dp, ϕ, t, β and E are the number of teeth, the module, the pitch diameter, the pressure angle, the width of gear teeth, the helix angle and the material modulus of elasticity, respectively. These gears selection do not precludes the use of others pairs of gears with the same center distance and that fit in the gearboxes

It was observed that the gears' internal diameter from the supplier has 8 mm. Then, the shafts were designed with an external diameter of 12 mm, because of the convenience of finding Ø12.7 mm steel bar in Brazilian industrial marketplaces. So the mechanical strength calculations were made for this configuration and they were published by Silva (2018). Also, the shafts were designed to be manufactured from stainless steel bars. Then, the shafts have simple geometry (with a diameter of 12mm through their whole length), and the components' placements were designed to be made with the aid of spacing bushings. Finally, the bearing housing which the shafts pass through counts on seal retainer to avoid oils leakage.

The gears housing were developed in order to accommodate the gears and oil. The redesigned gearbox is composed basically of the gear housing and two bearing housings sealing. Thus, the bearing housings are intended to support the shafts with their assembled components, and the gear housing has the purpose of accommodating the gears and serve as an oil sump. So, the gearboxes setup can be visualized in Fig. 2

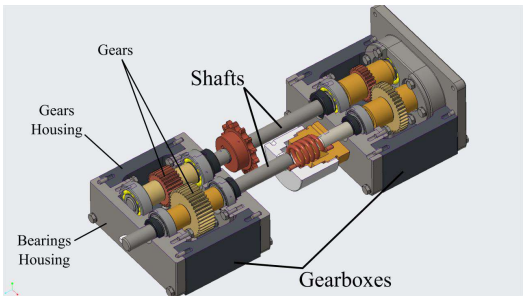


Figure 2. Sectioned view showing the setup of the proposed reduced FZG gearboxes and shafts

In order to obtain a piece of reliable equipment avoiding assembling mismatch, the shafts have to work as most aligned as possible and maintaining the center distance and the parallelism between each other. Therefore, the four rolling bearings of each shaft need to be mounted coaxially between them and perpendicularly to the main external surface of the bearing housing. Especially thoughts have to be taken during the machining, and these cares are foreseen in the design of the components. Both bearings housing and the gears housing have tight dimensions and geometric tolerances to allow the expected work conditions (according to Fig. 3).

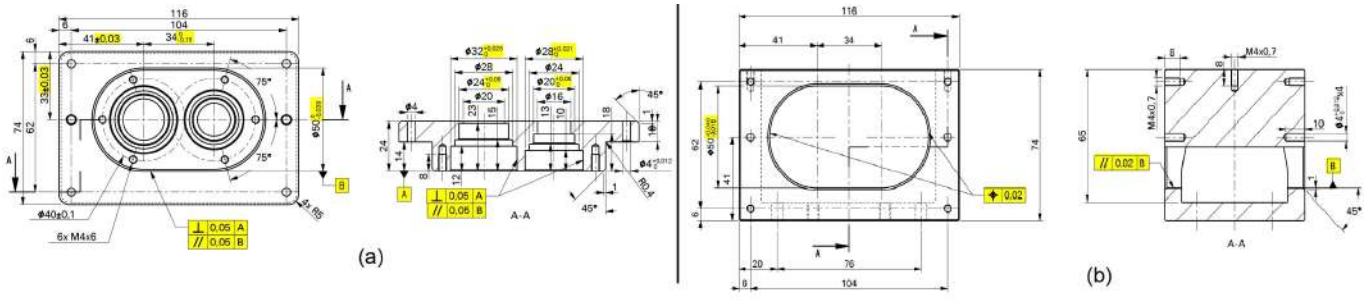


Figure 3. (a) Technical drawing of the bearing housing with emphasis on dimensional and geometric tolerances; (b) technical drawing of the gear housing with emphasis on dimensional, geometric and position tolerances

Gears lubrication mode will be the splash lubrication, where the oil level covers part of the gear, which is responsible for carrying the lubrication oil to the pinion. The oil level shall be up to three times the gear teeth high, i.e., 6,5 mm of the gear shall be immersed in oil. The gearbox was modeled using a CAD system with the lubricant oil inside (up to the suggested level). Then, the oil volume could be estimated through the CAD measurement function that measures the oil model volume and the interference volume between the oil model and the others. So the accurate oil volume is the difference between the oil model volume (i.e., 88342.3 mm³) and the interference volume (i.e., 13981.5 mm³) (see in Fig. 4). Then, the estimated oil volume is 74360.8 mm³ or 74.36 ml.

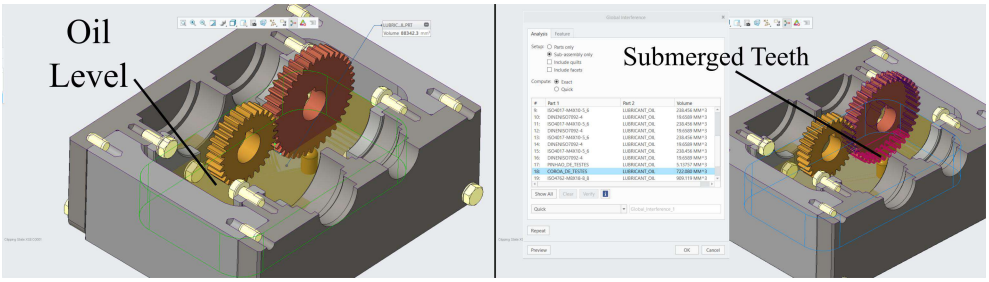


Figure 4. Estimation of the required oil volume to lubricate the proposed reduced FZG gearboxes.

## 4. METAL FRAME

The original FZG tribometer is assembled on a one-piece manufactured base. This configuration is susceptible to versatility issues (such as adding new components to the tribometer or correcting any unexpected error during the design phase). However, a more versatile base was designed considering the ease of adding or removing subsets. An adequate solution for the problem presented was replacing the one-piece base with a metallic structural aluminum frame. The structure was conceived, designed, and assembled on the CAD platform based on Forseti's components (2021). The main components of the structure are aluminum profiles (and their variations) and the so-called universal connectors (according to Fig. 5). Although Linden (2014) uses a milled plate with “T” grooves on the aluminum profiles, only aluminum alloy profiles were used in this propose (for the sake of financial feasibility). However, this kind of mechanical design allows for the expansion of subsystems and improvements, even in the base structure.

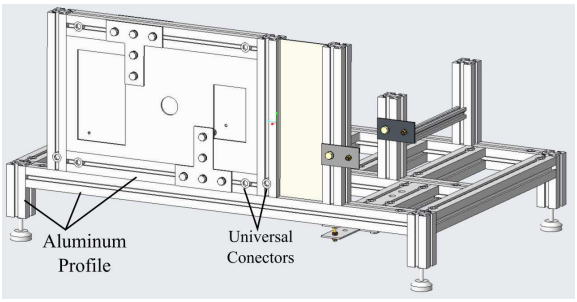


Figure 5. 3D CAD model of the metallic structure that supports (in the mechanical design) the reduced FZG tribometer.

Selected aluminum profiles have a 0.5 AlMgSi chemical composition (6063 aluminum alloy). Furthermore, the profiles have channels and faces through which it was possible to assemble components with special screws and nuts. The joints between structured profiles were designed with the use of universal connectors. Universal connectors consist of an internally threaded bushing, a grub screw, a spring, and a pin. The bushing is mounted inside the holes (18 mm) found at the ends of aluminum profiles. The bolt and spring regulate the depth of the pin in the bushing, and the fitter can adjust this depth by tightening or loosening the bolt. The pin has a protruding end whose function is to be mounted in the channels of the profiles. As the universal connector screw is tightened, the pin clamps the end of the profile against the face of another profile forming a rigid joint. The arrangements of the profiles (aluminum bars) can be adjusted by loosening and tightening the universal connector screws, bringing the bars closer or further apart as needed. Aluminum bars can also be added or removed from the assembly featuring a versatile, rigid, and fully adjustable structure (as shown in Figure 6a, 6b, 6c, 6d, and 6e). The aluminum alloy structure has specific locations for assembling each sub-assembly. For example, it can mention the 40 mm x 80 mm profiles designed to receive the gearboxes. The control panel (where the electrical control system is located) is also designed to face the machine operator. Meanwhile, for safety reasons, the loading system is designed to be mounted on the back of the tribometer. It is important to note that the brake disc (190 mm) rotates at high speed, which can be a risk to the operator. On the other hand, to make the

workflow easy, the place to input standard masses is located in front of the system. This position allows for quick operator access, which is shown in Fig. 6f.

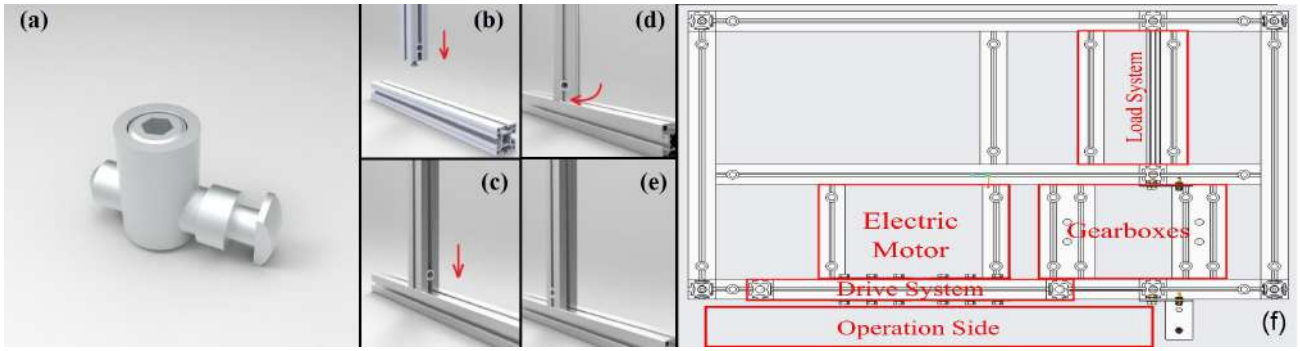


Figure 6. (a) Universal connector; images (b), (c), (d) and (e) illustrate the ease of assembly and versatility of universal connectors; and (f) arrangement of sub-assemblies on the aluminum structure.

## 5. LOAD SYSTEM AND HERTZIAN STRESS ON THE GEARS TEETH

It was necessary to redesign the loading system to accelerate wear on the gear teeth and solve the static load problem (present on the original FZG tribometer). A loading system based on a disc brake and a brake caliper activated by standardized masses pieces was planned as an alternative. The new loading system consists of a system with a caliper and brake disc mounted on an axis parallel to the principal axes of the tribometer. The brake caliper, driven by a steel cable with standard masses at its end, presses (with two brake pads altogether) the disc and, by friction, applies a braking force to the disc. The torque generated by these described components is transmitted to the shaft by a flange. Successively, the loading shaft transmits the torque, by chains and sprockets, to the driven shaft of the tribometer, according to Fig. 7.

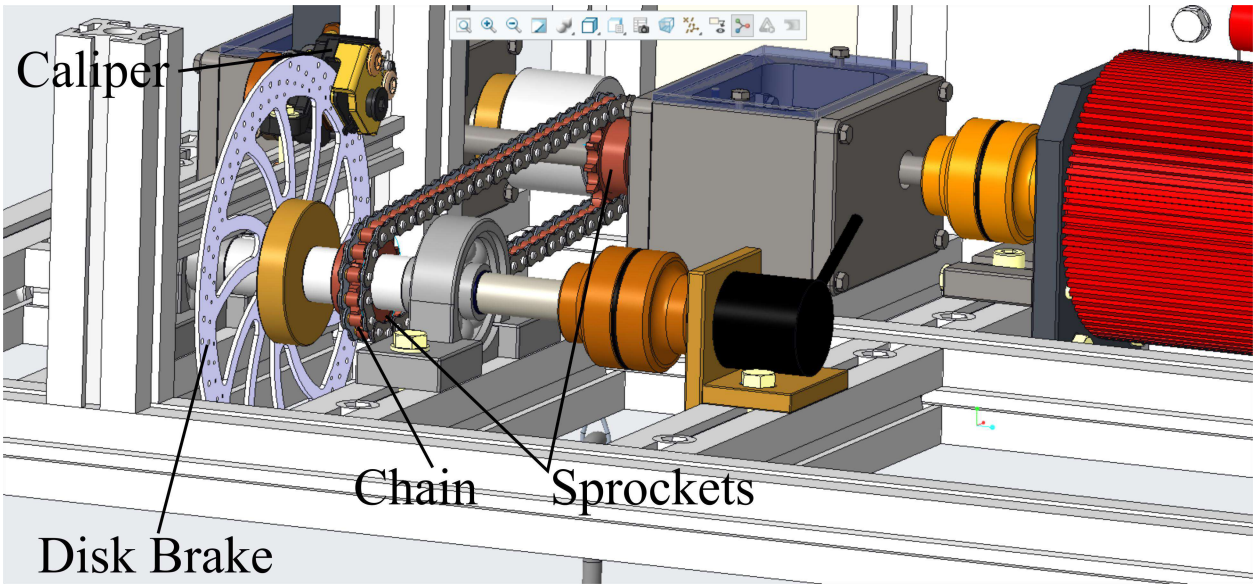


Figure 7. Image of loading system of the proposed FZG tribometer.

Unlike the tribometer presented in DIN ISO 14635-1 (2000), which brings a loading system directly coupled to the driven shaft, this proposed design has a loading system designed on a third axis, external to the gear train axes. Thus, it will be possible to assemble measuring instruments and new subsystems to apply improvements to the device using the free shaft ends in the loading system (as can be seen in Figure 8). The use of an external loading system (the drive and driven axes) calls into question the need to use a drive gearbox. However, in more advanced studies, this back-to-back configuration makes it possible to use both gearboxes as test boxes for simultaneous tests. Furthermore, the back-to-back format also allows cylindrical helical gears without changes in the bearings (since tested gears have the same helical angle).

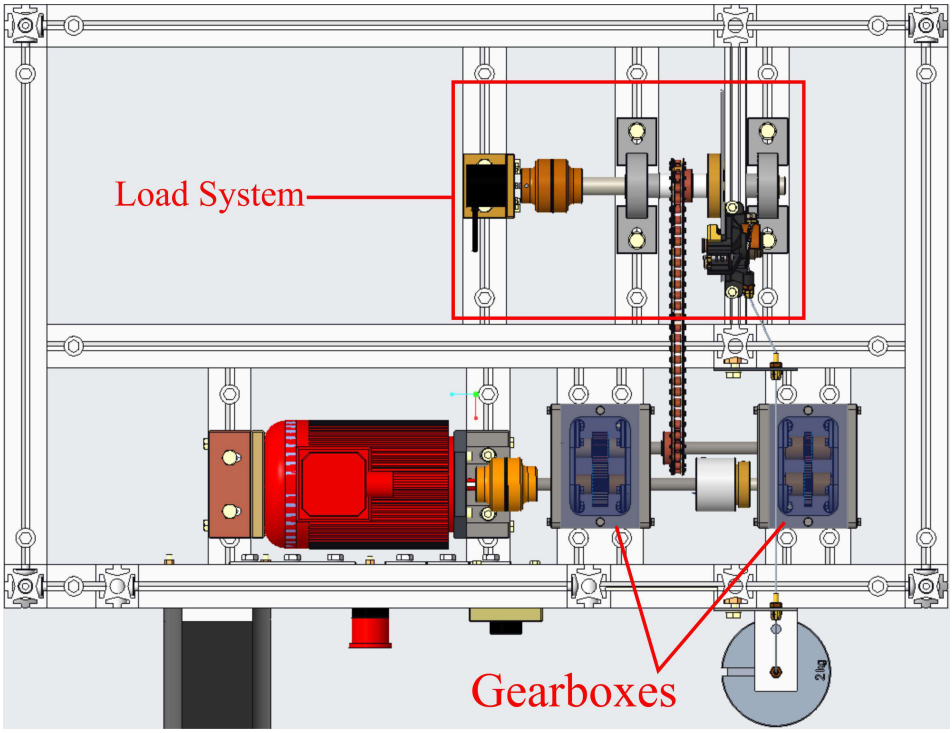


Figure 8. Top view of the proposed FZG tribometer with an emphasis on the arrangement of the charging system components.

According to Norton (2010), the torque transmitted to the shaft by the braking force of a brake disc can be defined as:

$$T_{brake} = n\mu_{brake}F_{pads}\frac{2\left(r_o^3 - r_i^3\right)}{3\left(r_o^2 - r_i^2\right)} \quad (1)$$

Where $T_{brake}$, $n$, $F_{pads}$, $\mu_{brake}$, $r_0$ and $r_i$ are the braking torque transmitted to the shaft, the number of contact faces between the brake caliper and the brake disc, the force applied to the brake pads, the friction coefficient between the brake pads and the brake disc, the distance between the center of the shaft and the end of contact with the brake pads and the distance between the center of the shaft and the beginning of contact with the brake pads, respectively.

Tribology Study Group at UFRN carried out pin-on-disk tests to determine the average friction coefficient of metallic and semi-metallic materials applied in brake discs and pads. The results obtained indicated an average friction coefficient equivalent to 0.343 (after 2000 s). A similar value was obtained by Orłowicz et al. (2016) in the investigation of the friction coefficient in the pin-on-disk contact. Moreover, the number of faces in contact with the brake disc is 2. Furthermore, the starting and ending radii for a brake disc diameter (180 mm) and a conventional bicycle brake caliper are 75.2 mm and 89.2 mm, respectively.

Finally, the force applied by the brake pads on the brake disc was calculated with the aid of real caliper brake and a helical spring assembled between the two brake pads. The spring constant was known as 245.25 N/m. Meanwhile, deflection values were measured from one pad to another using the claws (for internal measurements) of a Mitutoyo pachymeter with a maximum length of 150 mm. Then, the measurements were carried out in two different opening positions of the brake caliper, the first opening without loading and the second with a 30 N load applied to the steel cable. Thus, five spring deflection measurements were taken for each brake caliper position and, subsequently, the average value for each deflection was calculated. The average value of the deflections was used to calculate the force applied by the pads on the brake disc and, consequently, the brake torque (see on Table 2 and Figure 9).

Table 2. Results of deflection measurements of the coil spring assembled between the brake pads and their correlation with the forces applied to the brake disc and the brake torque.

| Measurement (mm) | 1 | 2 | 3 | 4 | 5 | Average | Applied Force (N) | Brake torque (Nm) |
|---|---|---|---|---|---|---|---|---|
| **No-load Position** | 9.15 | 9.05 | 9.10 | 9.00 | 8.90 | 9.04 | 0.00 | 0.00 |
| **Load Position** | 7.05 | 7.25 | 7.15 | 7.25 | 7.30 | 7.20 | 0.45 | $2.53 \times 10^{-2}$ |

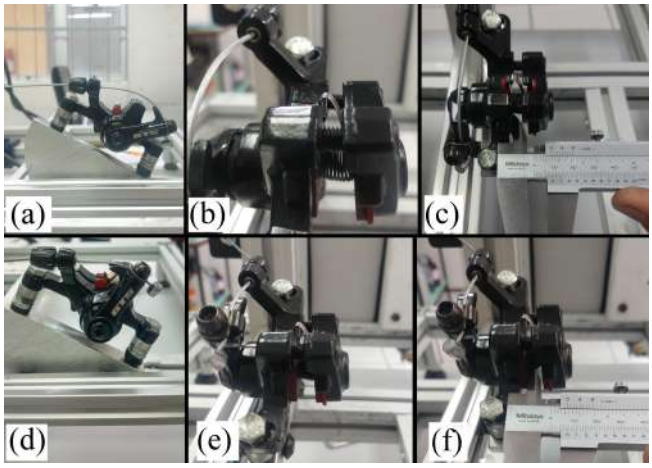


Figure 9. (a) no-load position of the brake caliper;(b) spring deflexion in no-load position;(c) spring deflexion measurement in no-load position;(d) load position of the brake caliper;(e) spring deflexion in load position;(f) spring deflexion measurement in load position.

## 6. TORSIONAL SPRING COUPLING

In order to ensure the engagement between the pairs of gears despite possible misalignments, a coupling with a torsion spring was developed to be coupled to the drive shaft. This coupling has the function of applying a pre-torque on the gears in order to ensure the contact between the gears. For this, the coupling was designed with three components: two coupling elements to the shafts and a torsion spring between them, whose torque (once twisted) must be greater than the torque provided by the motor shaft.

As can be seen in Figure 10, the coupling consists of three components and two M4x0.7 x 6 mm headless hex head screws. The white and gold colored components are the coupling elements to the shafts, while the red element is a torsion spring.

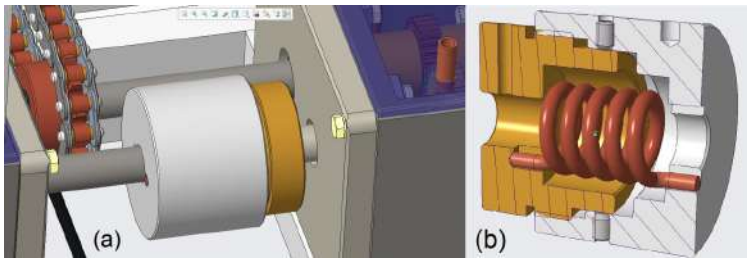


Figure 10. CAD model of (a) spring-loaded coupling mounted between drive shafts; and (b) mechanical torque limiter in full section.

The coupling elements are assembled together using two references: (1) the smallest external diameter of the golden element has a nominal dimension equal to the second largest internal diameter of the white element (these diameters were called guide diameters); (2) the largest inner diameter of the white element is an M42x2 thread which must be fitted to the outer thread of the same dimensions as the intermediate outer diameter of the gold element. In this way, the coupling is guided by a sliding fit between the inner and outer diameters of the gold and white elements (respectively).

Threaded mounting ensures that the shafts can rotate around their axis, but consideration must be given to fixing the couplings to the shafts. One of the coupling elements (the white element) is designed to be keyed to the shaft in order to transmit power. Similarly, the golden coupling element was designed so that the transmission of torque and angular movement for the coupling is carried out with the aid of a headless allen screw, whose tightening will imply the application of a load on the shaft surface.

Between the coupling elements there is a torsion spring. When assembling the three elements as shown in Figure 11 (b), the golden coupling element must be twisted with the aid of a cylindrical wrench while the white coupling element remains fixed. The torque applied for twisting the coupling must be: (1) in the opposite direction to the torque applied by the motor; and (2) of magnitude greater than the torque applied by the motor to Drive Shaft 1. The torque applied to the coupling is stored in the torsion spring as a form of elastic potential energy. The spring, in turn, applies torque to Drive Shaft 2 in order to force engagement between the test gears. Thus, once the motor starts, the spring torque must not be exceeded by the motor torque and the preload applied before the motor starts is sufficient to maintain the gear.

For deflections of up to 15°, the spring must provide a recovery torque slightly greater than the motor torque and in case of overload of the motor on the system, the spring must dampen the excess torque and signal (through markings on the face of the limiter) that the motor torque exceeded the spring deflection torque. However, this spring-loaded coupling can work with the objective of increasing the Hertz tension on the gear teeth and, for this, the coupling must be mounted to the drive shafts with a deflection of between 15° and 90°.

In order to maintain the preload on the gear teeth even after the motor started, it was necessary to design a spring capable of providing a higher torque than the motor. Thus, the Murphy & Read Spring Mfg (2021) virtual catalog was used for torsion springs, in which information such as: spring type, dimensions, torque supplied by the spring, deflection necessary to obtain the informed torque, etc., can be found.

Taking into account that the torque given by the engine can be calculated from the following equation (NORTON, 2010):

$$T_{motor} = \frac{H}{\omega_{motor}} \tag{2}$$

Where $T_{motor}$, $H$ and $\omega_{motor}$ are the torque provided by the electric motor, the power of the electric motor and the angular velocity on the motor shaft respectively.

Considering that the engine speed is 104.72 rad/s and the electric motor power is 145 W, then the torque provided by the electric motor is 1.385 Nm.

Thus, in view of the data presented and considering the durability of the product, a stainless steel torsion spring with reference #MT135-01-RH-MW from Murphy & Read Spring Mfg (2021) was chosen.. This spring is capable of providing a torque equal to 1.66 Nm for a 15° rotational deflection.

## 7. ELECTRIC MOTOR DRIVE SYSTEM

The electrical control system of the reduced FZG tribometer was designed with the objective of making starts and stops in a safe way. For this, a control system was designed using a 220V Schneider LC1E09 contactor, which is activated by an Altronic BDA-CI start/stop pushbutton.A schematic diagram can be seen in Figure 11, where it is clear the use of two independent energy networks, namely: i) the single-phase network for activating the on/off commands; ii) and the three-phase network for power supply and motor control.

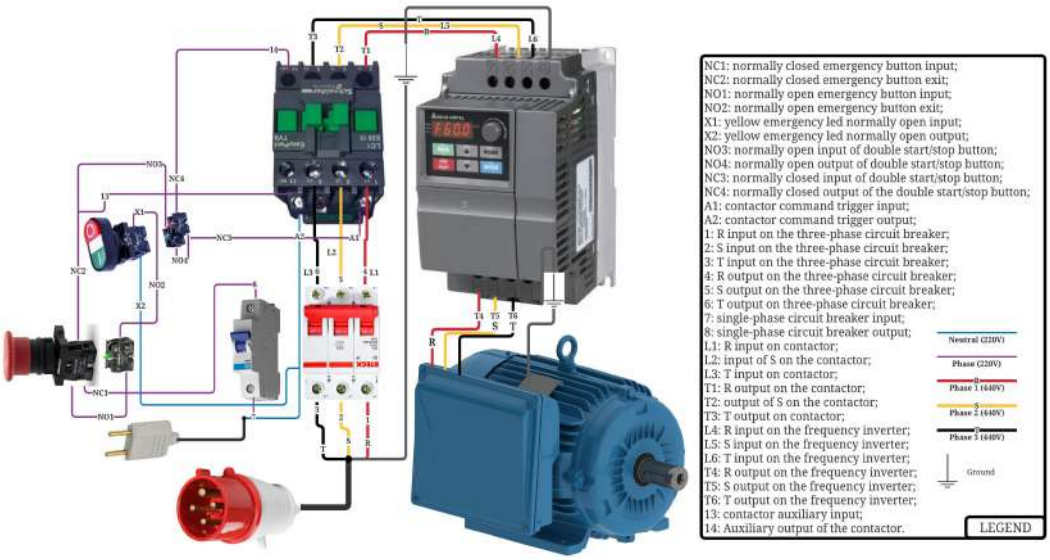


Figure 11. Illustrative diagram of the electrical control system of the reduced FZG tribometer.

The control system must be protected by a Tramontina TR6kA C6 single-phase circuit breaker and, in an emergency, the system has an Altronic BEA-GD emergency stop button. Activating the emergency button disarms the contactor, interrupts the contact of the three-phase network with the motor and turns on a yellow emergency LED. The contactor can only be activated again when the contact on the emergency button returns to normally closed.

The electric motor designed to be powered by the three-phase network (380V~440V) is controlled by the WEG CFW 09 frequency inverter. The phase cables, in principle, pass through a Steck SD 3P C10 three-phase circuit breaker, subsequently, supplying the contactor, which, when On, it supplies the frequency inverter.

## 8. TRIBOMETER POWER FLOW AND HERTZIAN STRESS ON GEAR TEETH

With the addition of the charging system, drive system and torsion spring coupling to the conceptual design, it was possible to perform a power flow analysis. For this, the input power (entered by the motor), the transmission ratio between the gears, the intermediate coupling torque and the brake disk braking torque (see Figure 12) must be considered.

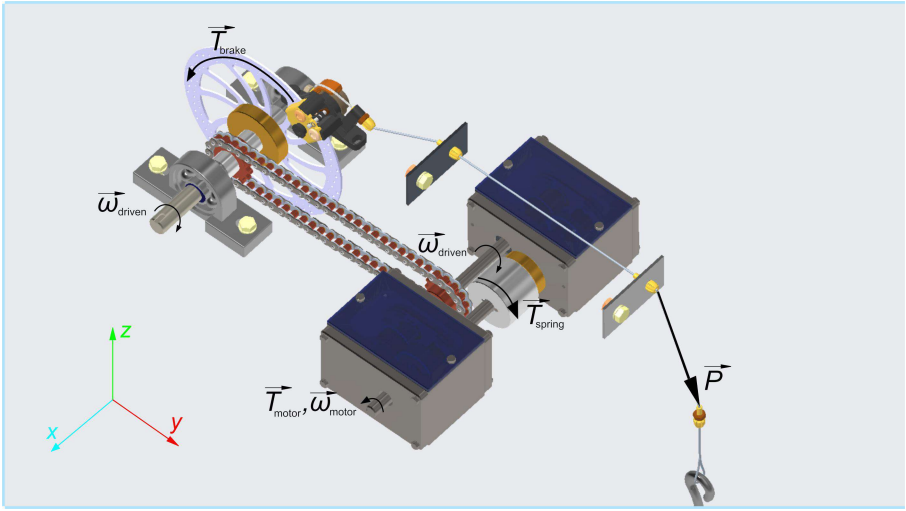


Figure 12. Power flow diagram of the reduced FZG.

Where, $\vec{T}_{motor}$, $\vec{P}$, $\vec{\omega}_{motor}$, $\vec{T}_{spring}$, $\vec{T}_{brake}$ and $\vec{\omega}_{driven}$ are the torque provided by the electric motor, the force applied by the weight pieces in the steel cable, the angular velocity on the motor shaft, the restoring elastic force of the torsion spring, the braking torque transmitted to the shaft of the load system, and the angular velocity on the load shaft respectively. From the analysis of the torques acting in the system, it is possible to determine the Hertz tensions present in the gears for each position of the brake caliper and its respective load.

The calculation of Hertz stresses starts from the definition of the normal load to the teeth. Norton (2010) sets the maximum normal load to gear teeth as:

$$W = \frac{2\sum T_{FZG}}{d_p \cos\phi} \tag{3}$$

Where $W$, $\sum T_{FZG}$, $d_p$ and $\phi$ are the maximum normal load to gear teeth, the sum of torques in the reduced FZG tribometer and the the pressure angle on the gear teeth respectively.

The sum of the torques in the reduced FZG tribometer includes: the braking torque; the motor torque; and the torsions spring torque. The braking torque is presented in Table 2 and has a value of 0.025 Nm. Meanwhile, the motor torque has a value of 1.385 Nm and the spring torque is equivalent to 1.66 Nm. To perform the summation, all positive signs of torque must be considered, as, analyzing Figure 13 and the sequence of torque application, it is noted that: 1) the spring torque has a negative direction on the X axis and is the first to be applied (still during assembly); 2) the braking torque has a positive direction on the X axis and resists the action of the spring torque on the test gears; 3) and, since the gear teeth are under the action of the braking and spring torques, the system is put in rotation under the effect of the motor torque. Thus, it is possible to infer from this analysis that the three torques are added to the action on the gear teeth. So, the sum of the torque takes on the value of 3.07 Nm.

Considering the values given in the item 3 about the gears geometry, the maximum normal load to pinion teeth assumes the value of 233.358 N. Then, it is possible to calculate the hertzian stress on the pinion teeth using the following formulation presented by ISO 6336:2014:

$$\sigma_0 = Z_H Z_E Z_\varepsilon Z_\beta \sqrt{\frac{W}{d_p t} \cdot \frac{u+1}{u}} \tag{4}$$

Where $Z_H$, $Z_E$, $Z_\varepsilon$, $Z_\beta$, $W$, $d_t$, $t$, and $u$ are zone factor, elasticity factor, contact relationship factor, helix angle factor, pinion primitive diameter, width of gear tooth, transmission ratio between gears respectively.

The formulation for each presented factor can be found on ISO 6336:2014 and all factors depend exclusively on the gears characteristics given on this work. Complementarily, the hertzian stress present on the pinion teeth can be calculated applying the values given in the item 3 and the value of the normal load on the pinion teeth. So, the maximum hertzian stress on the pinion teeth equals 90.743 MPa.

## 9. PROJECT OVERVIEW AND CONCLUSIONS

The proposed reduced FZG design was concluded with eight subassemblies, i.e., the metal frame, the driven shaft, the torsional spring coupling, the drive shaft 1, the drive shaft 2, the gearboxes, the load system, and the electric motor drive system. The proposed mechanical design also predicts the mounting of a monitoring system, which will have three different types of transducers: a thermocouple mounted on the bottom of each gearbox; an accelerometer mounted on the sidewall of each gearbox; an encoder mounted on the load shaft. They will monitor the oil temperature inside the gearboxes, the gearboxes' vibrations levels compared with the advance of wear, and the rotational position and velocity throughout the test.

So, it is possible to conclude that the proposed design meets the prerequisites presented and can promote wear on gears teeth, testing the efficiency of lubricants or the strength of the gear to contact fatigue. Finally, this project's execution shall follow two strands: the purchase of the standardized components (include in the project intentionally to facilitate the construction phase) and the machining of the components exclusively designed for this project.

## 10. ACKNOWLEDGEMENTS

This study was financed in part by the CNPq (National Council for Scientific and Technological) and the Coordenação de Aperfeiçoamento de Pessoal de Nível Superior - Brasil (CAPES) - Finance Code 001.

## 11. REFERENCES

ABEEólica, 2019. *ABEEólica Numbers, February 2019* (in Protuguese). Associação Brasileira de Energia Eólica (ABEEólica), São Paulo, http://abeeolica.org.br/wp-content/uploads/2019/02/N%C3%BAmeros-ABEE%C3%B3lica-02.2019.pdf. Accessed 23 September 2019.

ATI Brasil, 2021, *Gears (in Portuguese)*, Artigos Técnicos Industriais Brasil, ATI Brasil, Curitiba, https://www.atibrasil.com.br/17-engrenagens. Accessed, 25 June 2021.

Carreteiro, R. P. and Belmiro, P. N. A., 2006. *Industrial Lubricants & Lubrication (in Portuguese)*. Editora Interciência Ltda., Rio de Janeiro.

Fernandes, C. M. C. G., Marques, P. M. T., Martins, R. C., Seabra, J. H. O., 2016. “Energy efficiency tests in a full scale wind turbine gearbox”. *Tribology International*, Vol. 101, pp. 375-382.

Forseti, 2021, *Virtual Store (in Portuguese)*, Forseti Soluções, Curitiba, https://www.loja.forsetisolucoes.com.br/. Accessed, 25 June 2021.

Linden, F.L.J. van Der, 2014. "Gear test rig for health monitoring and quasi static- and dynamic testing; design, construction and first results". In *Proceedings of International Gear Conference*. Lion, France.

Manoj, V.; Gopinath, K.; Muthuveerappan, G., 2015. *Development of a Power Re-Circulating Gear Test Rig*, Indian Istitute of Technology Madras, Chennai, http://www.nacomm03.ammindia.org/Articles/Mac007.pdf. Accessed 17 June 2021.

Murphy & Read Spring Mfg, 2021, Murphy & Read Spring Manufacturing Co., Murphy & Read Manufacturing Co., Philadelphia, https://www.mrspring.com/. Accessed, 25 June 2021.

Norton, R. L., 2010. *Machine Design: An Integrated Approach*. Prentice Hall Pearson, 4th ed..

Orłowicz, A.W., Mróz, M., Wnuk, G., Markowska, O., Homik, W., Kolbusz, B., 2016. "Coefficient of Friction of a Brake Disc-Brake Pad Friction Couple". *Archives of Foundry Engineering*, Vol. 16, pp. 196-200.

Santos, F. P., Teixeira, Â. P.; Soares, C. G., 2016. “Operation and Maintenance of Floating Offshore Wind Turbines”. *Floating Offshore Wind Farms.* Springer International Publishing, pp.181-193.

Spinato, Fabio, P.J. Tavner, G.J.W. van Bussel, E. Koutoulakos, 2009. “Reliability of wind turbine sub-assemblies”. *IET Renewable Power Generation*, Vol. 3, No. 4, pp. 1-15.

Silva, L. M. de C., 2018. *Mechanical Design of a Contact Fatigue Tribometer - Reduced FZG* (in Portuguese). Graduation Monograph, Mechanical Engineering Department, Federal University of Rio Grande do Norte, Natal, Brazil.

## 12. RESPONSIBILITY NOTICE

The authors are the only responsible for the printed material included in this paper.